American-Eurasian J. Agric. & Environ. Sci., 8 (3): 339-348, 2010
ISSN 1818-6769

Forest Fires and Follow-up Rehabilitation in the Gallipoli National Historical Park Area 1986 Forest Fire Case

[1]*Rüstü Ilgar,* [2]*Muzaffer Özdemİr*

[1]Department of Çanakkale Onsekiz Mart University,
[2]Faculty of Education, Geography, TR- 17100 Çanakkale-Turkey

Abstract: 1986 forest fire in Gallipoli Peninsula National Historical Park (GHP) area, the vegetation cover changes have been monitored by use of multi-temporal images selected from different satellites and sensors such as Landsat (with MSS, TM, ETM) and Aster satellites. 9 images were acquired in 1982, 1987, 1992, 1998, 1999, 2001 and 2007 for the analysis. We applied the Change Vector Analysis and Tasseled Cap. Transformations in order to determine the changes in the amount of vegetation cover in the forest-fire area. Areas which show "change" and "no change" in the difference images were obtained by using the Change Vector Analysis. Changes were then calculated through a threshold value determined by the Expectation Maximization (EM) Algorithm. At one stage of analysis, it was quite difficult to distinguish the reforestation-preparation areas from the newly-burnt fires, in the Landsat data. NDTI= [(TM 5-TM 7)/ (TM 5 + TM 7)]. Here by, TM5 and TM7 are the reflectances in the Landsat TM5 (1550-1750 nm) and TM7 (2080-2350 nm) bands, respectively. Figure 10 is a representation of frequency distribution of NDTI values for the image under consideration. The analysis shows that NDTI ≤ 5 (positive values near zero or all negative values of the index) correspond to recent forest fires while NDTI > 5 (larger positive values) regions are the reforestation-preparation areas.

Key words: Remote Sensing · Temporal Change Analysis · Change Vector Analysis · Normalization · Expectation Maximization Algorithm · Tasseled Cap Transformation

INTRODUCTION

The main aim to find out the extend of temporal changes as well as vegetation recovery rates for a 25 year-long period of 1982-2007, after a forest fire in 1986 in Havuzlar Region of Gallipoli Peninsula National Historical Park (GHP) located on the southern end of the Gallipoli Peninsula on the European side of the Dardanelles Strait. The GHP itself covers an area of 33000 hectares in the southern part of Gallipoli Peninsula. Natural and historical assets in GHP are under serious threat due to the high density of visitors (from abroad and from Turkey) and the existence of agricultural lands within and/or by and near the forest lands. The latter is also considered as the main cause of frequent forest-fires in the GHP.

MATERIAL AND METHOD

Study Area: The study area (Havuzlar Region) lies on the southeast side of GHP with an approximate area of 9115 ha. The position and general appearance of the region at different dates in the Landsat TM 7, 4, 2 and Aster 2, 3, 1 band combinations can be followed from Figure 1.

Satellite Images and Analysis Platforms Used in the Study: The data set used in the present study consists of 9 satellite images of the area acquired at different dates between 1982- 2007 (Table 1). All bands (except thermal band 6) of Landsat (MSS, TM, ETM) images and bands 1,2 and 3N of Aster Satellite images were used in the analysis. Image analysis and assessment work were carried out by PCI Geomatica, ArcGIS and Matlab 6.5 software platforms.

Preprocessing: Comparing between images, there are potential source of errors in a change analysis as change in illumination and atmospheric conditions between the two acquisitions; also they can have pixels with different coordinates for the same area on the ground. To solve these problems, radiometric calibration and co-registration

Corresponding Author: Rüstü Ilgar, Department of Çanakkale Onsekiz Mart University, Faculty of Education, Geography, TR- 17100 Çanakkale-Turkey, E-mail: ilgar@email.com.

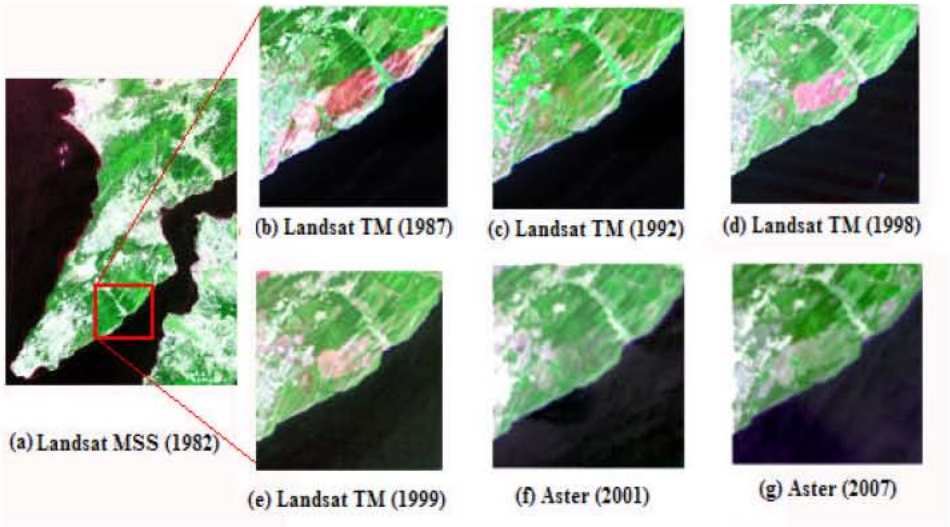

Fig. 1: A long haul optical WDM network map [1]

Table 1: Images used for the present analysis

	Satellite Images Used	Date of Acquisition
1	Landsat MSS	September 01, 1982
2	Landsat TM	July 21, 1987
3	Landsat TM	April 22,1992
4	Landsat TM	July 12, 1998
5	Landsat TM	August. 08, 1999
6	Landsat ETM	July 25, 2000
7	Landsat ETM	August. 20, 2001
8	Aster	August. 13, 2001
9	Aster	August. 21, 2007

should be used [2]. Different methods can be processed for relative corrections such as histogram adjustment, dark-pixel subtraction and multi date normalization using a regression model approach [3]. In the multi-date normalization method, pixel intensity values in one image were normalized to have the same mean and variance as those in the other [4] to remove most of the illumination and atmospheric effects. We applied relative radiometric corrections for which help to remove or normalize the variations within a scene and normalize the intensities between the images.

Tasseled Cap Transformation: The Kauth-Thomas transformation, usually shortened as Tasseled Cap (TC) Transformation was initially developed for crop-development surveys, in which three orthogonal indices called brightness, greenness and wetness are obtained for each band of satellite image [5-7]. While brightness measures soil brightness or total reflectance, greenness component is a measure of contrast between the near-infrared and the visible bands. The last component wetness represents the amount of moisture and contrasts the sum of the visible and near-infrared bands with the sum of the longer-infrared bands [8]. Tables 2, 3, 4 and 5 indicate TC coefficients of the brightness, greenness and wetness (for MSS, yellowness) for MSS, TM, ETM of Landsat and also Aster bands.

Change Vector Analysis: "A 'change vector' is a useful tool for monitoring the changes in region and defined by a measurable magnitude, characterizing the intensity of change and by a direction, characterizing the nature of such a change in the spectral space" [11].

Change vector analysis (CVA), represent all the information contained in the spectral change vectors acquired with the subtraction of corresponding spectral bands of two images taken at different dates, used in an empirical way without referring to a specific theoretical framework capable to properly [12]. Change vector magnitude (|M|), identified by computing and analyzing the modulus of change vector, is measured as the sum of the "Euclidian" separations of brightness values between two different times (t1 and t2) as;

$$M = \sqrt{\sum_{i=1}^{n} (b_i^{t2} - b_i^{t1})^2} \quad (1)$$

here b_i 's are brightness values of single bands of images (i=1...n).

On the other hand, change vector direction, gives information about the kind of change, is specified for each possible combination of negative or positive changes for each input band. This result in 2n possible change vectors possible for each pixel, where n is the number of input bands [13-15].

Table 2: Tasseled Cap Coefficients for Landsat MSS [11]

Index	MSS BAND1	MSS BAND2	MSS BAND3	MSS BAND4
Brightness	0.32331	0.60316	0.67581	0.26278
Greenness	-0.28317	-0.66006	0.57735	0.38833
Yellowness	-0.89952	0.42830	0.07592	-0.04080

Table 3: Tasseled Cap Coefficients for Landsat TM [5]

Index	TM1	TM2	TM3	TM4	TM5	TM7
Brightness	0.3037	0.2793	0.4743	0.5585	0.5082	0.1863
Grenness	-0.2848	-0.2435	-0.5436	0.7243	0.0840	-0.1800
Wetness	0.1509	0.1973	0.3279	0.3406	-0.7112	-0.4572

Table 4: Tasseled Cap Coefficients for Landsat 7 ETM+ (at-satellite reflectance) [10]

Index	TM1	TM2	TM3	TM4	TM5	TM7
Brightness	0.3561	0.3972	0.3904	0.6966	0.2286	0.1596
Grenness	-0.3344	-0.3544	-0.4556	0.6966	-0.0242	-0.2630
Wetness	0.2626	0.2141	0.0926	0.0656	-0.7629	-0.5388

Table 5: Tasseled Cap Coefficients for Aster (at-sensor radiance) [20]

Index	Aster Band1	Aster Band2	Aster Band3N
Brightness	-0.274	0.676	0.303
Greenness	-0.006	-0.648	0.564
Wetness	0.166	-0.087	-0.703

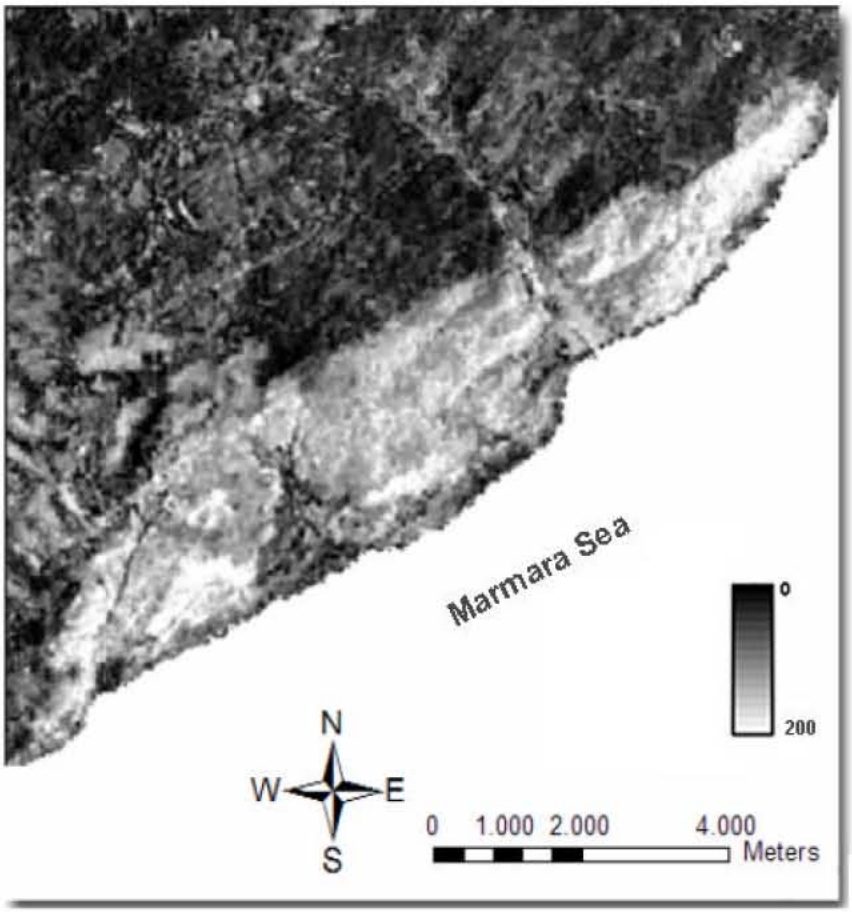

Fig. 2: The image obtained by the change vector magnitude (M) at each pixel position of brightness and greenness components of images 1 and 2 in Table 1. (The gray scale at right above correspond the gradual change of vector magnitude. The region within Marmara, sea region is not included in the analysis).

Decision Threshold: In order to decide that there is a change, the magnitude of the computed spectral change vector should be greater than a specified threshold criterion [2, 13, 16] have proposed that Expectation Maximization (EM) algorithm automatically identify the changes in difference images.

The EM algorithm is widely used for computing maximum-likelihood estimates for such data. Each iteration of the EM algorithm has two steps; the expectation step (E-step) and the maximization step (M-step). While the first step is computed with respect to the unknown underlying variables, using the current

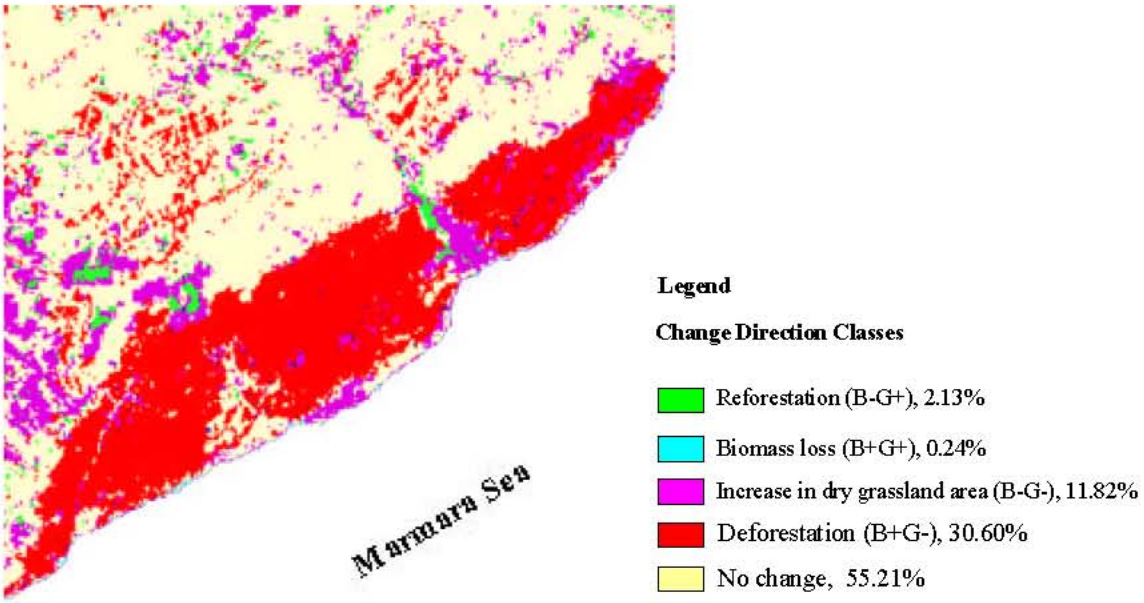

Fig. 3: A sample of variation of change vector magnitude values and the position of the threshold value (Th=52 for Figure 2 obtained using the EM algorithm).

estimates of the parameters and is conditioned by observations; the other one provides new estimates of the parameters [17].

Application: The material presented and methods summarized above were used to explore the 1986 forest-fire in the GHP area. As an initial measure of land cover-land use (LC/LU) changes in the study area, CVA, TCT and EM algorithms between two subsequent dates (starting with 1982 and 1987) were applied, changes in this region were followed in the same way until 2007.

For a CVA, the brightness and greenness components of selected 2 images were noted. The "change" / "no change" areas in the resultant "difference-image (Figure 2) were obtained. A threshold value (Th) was determined by the EM algorithm from the change magnitude distribution (Figure 3), using the Matlab codes [18]. To get the information about the kinds of change belonging to study area, the change vector directions in connection with the change classes were obtained using the rules shown in Table 6.

Positive changes in greenness (G+) indicate an improvement in vegetation cover area, while positive changes in brightness (B+) point to an increase in bare soil area. Negative changes for both indices (B- and G-) represent a decrease in bare soil and green vegetation cover areas respectively. The same pairs of values (brightness and greenness) were used to obtain the direction classes. Table 7 shows the possible change direction classes and their short description obtained from a CVA for indicated pairs of values.

Table 6: Inequalities used to determine the direction classes concerning the change classes. Here, M is the change vector magnitude, Th is the threshold value, B and G are the values of digital numbers (DN) proportional to the brightness and the greenness components of images taken at different times (t1 and t2)

Algorithm			Change Classes
If M >=Th and	B(t2) - B(t1) < 0 and G(t2) - G(t1) > 0	then	(B- G+)
	B(t2) - B(t1) > 0 and G(t2) - G(t1) > 0		(B+ G+)
	B(t2) - B(t1) < 0 and G(t2) - G(t1) < 0		(B- G-)
	B(t2) - B(t1) > 0 and G(t2) - G(t1) < 0		(B+ G-)

Table 7: Possible change direction classes in CVA and their description

Change Direction Classes	Description
B+G+	Biomass loss
B+G-	Decrease of forest vegetation cover
B-G+	Increase of forest vegetation cover
B-G-	Increase in dry grassland area

RESULTS

Application of CVA results in the total area of study region which shows a change above the determined threshold value are summarized in Figure 4 and Table 8.

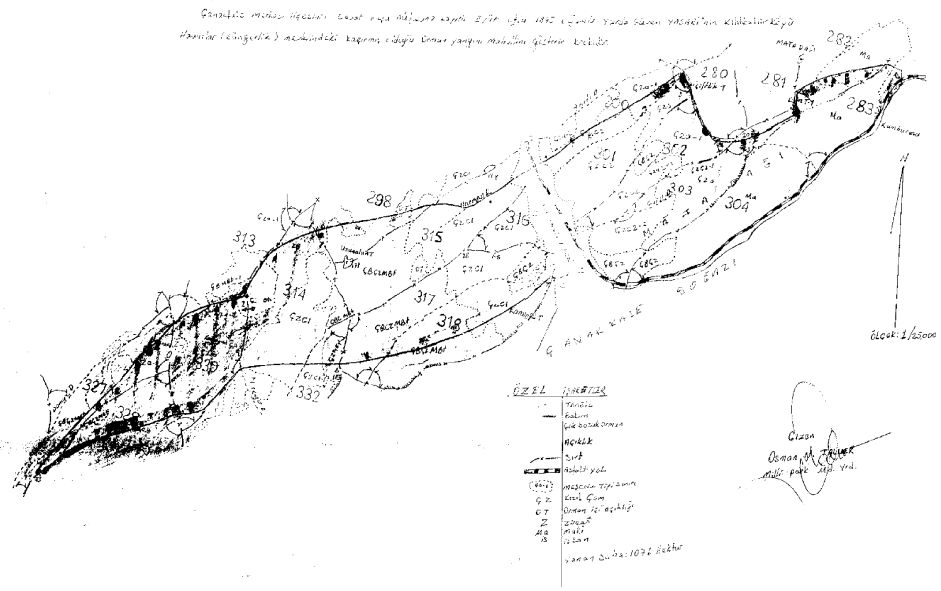

Fig. 4: Changes in greenness and brightness occurring in GHP Havuzlar Region from 1982 to 1987. The region within Marmara Sea region is not included in the analysis (According to official blank decision).

Table 8: Areas (ha) and percentages of changes occurring in GHP Havuzlar Region from 1982 to 1987.

Change Classes	Description	Area (ha)	Percent (%)
B- G+	Biomass loss	104.29	2.13
B+G+	Decrease of forest vegetation cover	11.53	0.24
B- G-	Increase of forest vegetation cover	578.08	11.82
B+G-	Increase in dry grassland area	1497.22	30.60
No Change	--	2700.97	55.21
	TOTAL	4892.09	100.00

Table 9: Areas (ha) and percentages of changes (%) occurring within study area for the 5 periods mentioned

Intervals	1982 to 1987		1987 to 1992		1992 to 1998		1999 to 2001		2001 to 2007	
Classes	Area (ha)	(%)	Area (ha)	(%)	Area (ha)	(%)	Area (ha)	(%)	Area (ha)	(%)
B-G+	20.0	1.2	1246.9	73.7	4.0	0.2	342.8	20.3	163.6	9.7
B+G+	6.7	0.4	175.7	10.4	40.0	2.4	18.8	1.1	87.1	5.2
B- G-	165.6	9.8	18.4	1.1	1.1	0.1	0.2	0.0	0	0.0
B+G-	1267.1	74.9	32.2	1.9	400.5	23.7	102.0	6.0	32.5	1.9
No Change	231.4	13.7	217.7	12.9	1245.3	73.7	1227.1	72.6	1407.6	83.3
TOTAL	1690.8	100	1690.9	100	1690.9	100	1690.9	100	1690.9	100

It was found that, between 1982 and 1987, 1497 (ha) of dense vegetation (30% of the total area) was lost. The bulk of fire area which we will concentrate on ignoring small patches within agricultural areas has a size of 1267. When the cause of the lost vegetation area was examined, it was deduced that it was due to the forest fire that occurred within our analysis dates. Indeed, a fire in the area began on August 14, 1986 and lasted about 54 hours according to Çanakkale Forest Management (ÇFM). A total of 1076 ha of forest area was lost, according to official records. Then, our estimation is about 25% larger than official estimation. The reason for this difference is not clear us. It could be that, there was a tendency not to include the half-burned or less than completely burned areas in the official fire records. As Figure 5 indicates, ÇFM map covers about the same area, but areal estimation is still much lower than the extent of fire areas in the satellite images.

Concentrating on the forest-fire area boundaries defined bulk red area in Figure 5 (which overlaps with ÇFM map), percentages of vegetation cover changes have been re-calculated and the same analysis is repeated for five change periods that can be defined with our data. Figure 6 summarizes the results of this exercise.

For the same change periods, Table 9 summarizes the areal sizes and percentage values for the entire project area. Same figures can be followed as a time series graph in Figure 7.

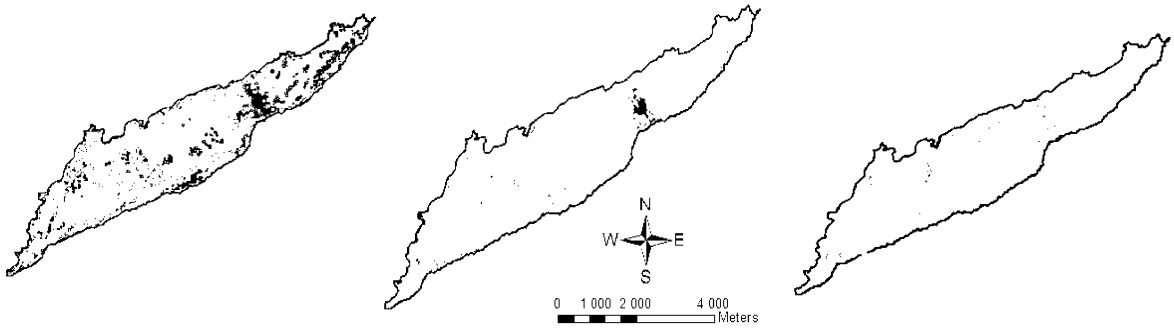

(a) 1982-1987 (extent of forest fire at Aug. 14. 1986)

(b) Changes in between 1987-1992

(c) Changes in between 1992-1998

Fig. 5: The map depicting the fire areas in GHP Havuzlar Region in 1986 according to Çanakkale Forest Management records. Areas burnt are indicated by parallel lines.

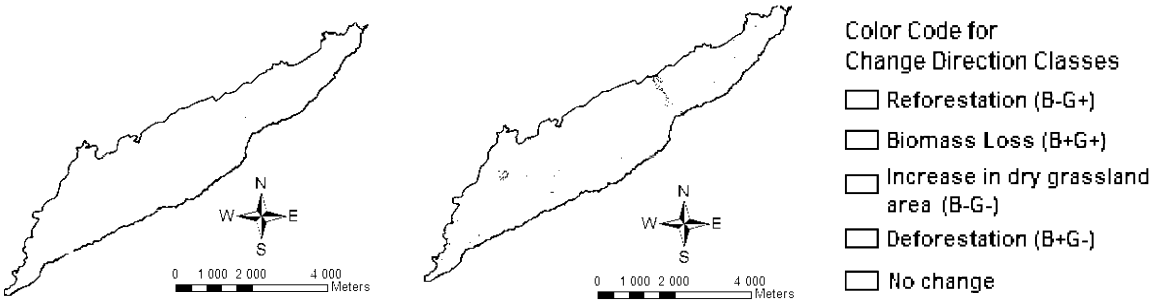

(d) Changes in between 1999-2001

(e) Changes in between 2001-2007

Fig. 6: Changes in G (greenness) and B (brightness) occurring in GHP Havuzlar Region for five change periods selected: (a) 1982-1987, (b) 1987-1992, (c) 1992-1998, (d) 1999-2001 and (e) 2001-2007.

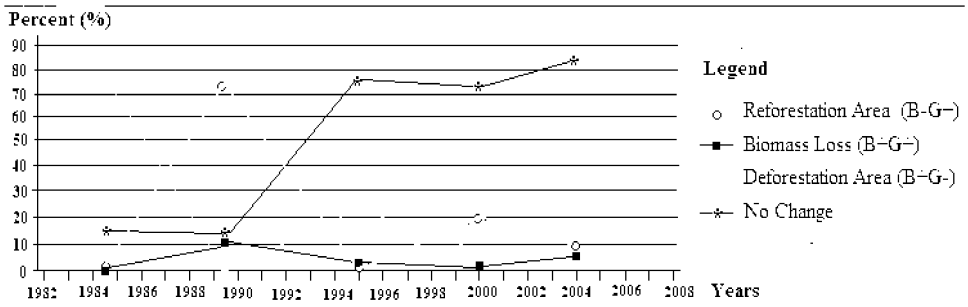

Fig. 7: Time series for various change vector values between 1982 and 2007. Parallel shapes of green (reforestation) and red (forest fire, i.e. deforestation) follow each other quite closely.

Changing in the amount of green vegetation cover in the next interval (between 1987 and 1992) were investigated, it was seen that more than 90% (1246 ha of 1267 ha) of burnt area has been recovered by a vegetation cover (Figure 6-b and Table 9). Same decrease in the amount of green vegetation in a small area is also visible in Figure 6-b. There is also, so called, the biomass loss of about of 10.4% (175.7 ha) of total which means that forest opening for agricultural and other purposes is of quite considerable amount especially onto deforestation Pinus brutia are.

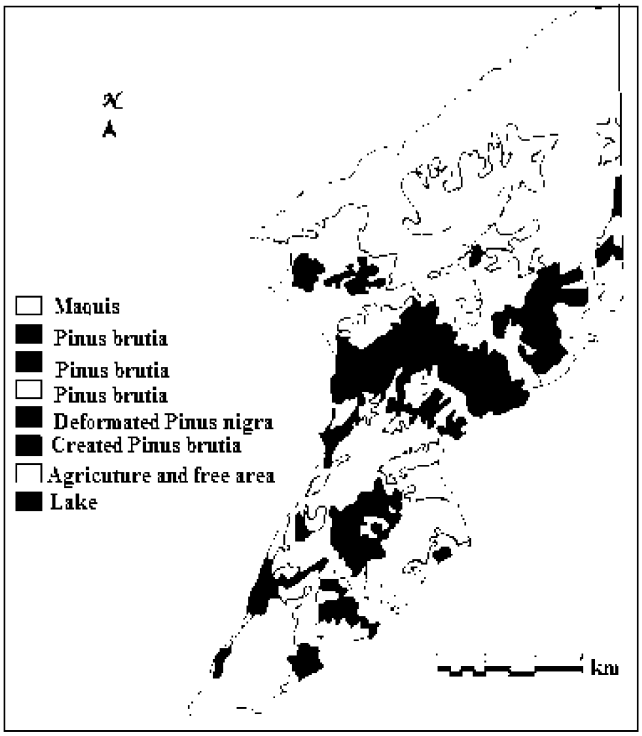

Fig. 8: Typ of Gelibolu Forest (Erten and all 2005)

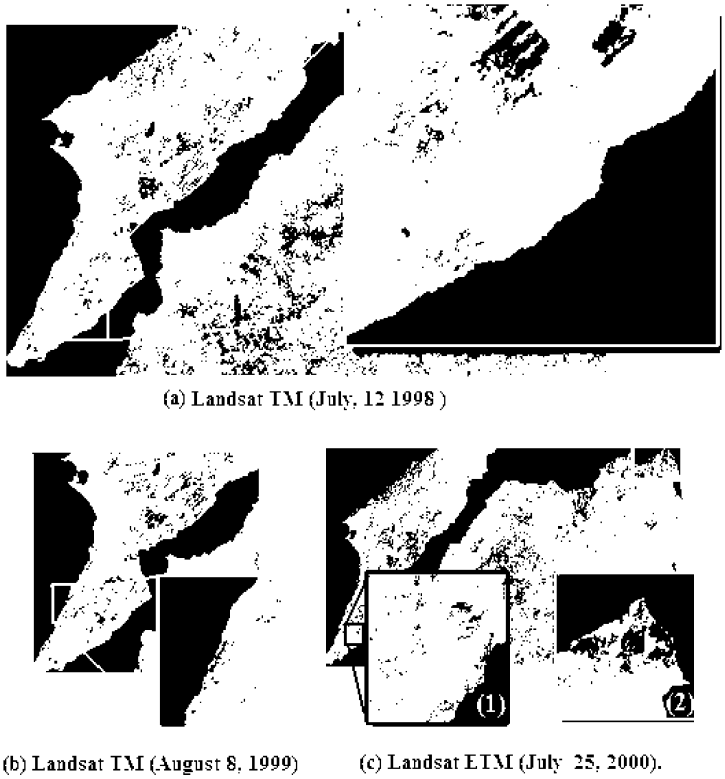

Fig. 9: Test areas in the Landsat images. (a) reforestation-preparation area for the earlier 1986 fire, (b) area of forest fire on July, 9 1999, (c) at left, another reforestation-preparation area for 1986 fire; at right, a new forest fire on July, 13 2000, on the same image, used to distinguish between the 2 classes under discussion.

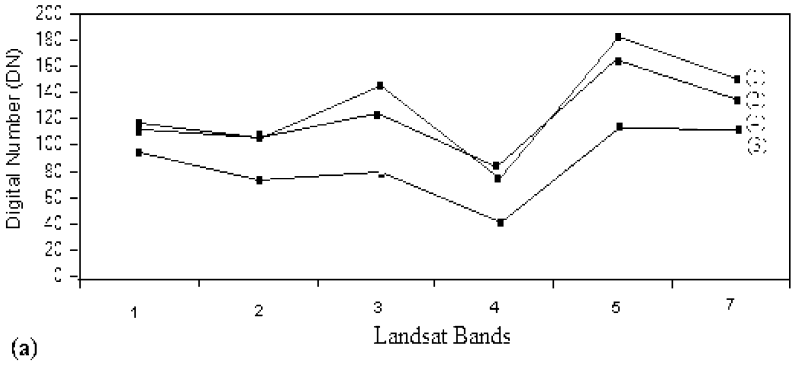

(a)

Legend

	Date	Defination	Used images
(1)	1998	Preparation for reforestation	Landsat TM July 12, 1998
(2)	2000		Landsat ETM July 25, 2000
(3)	July 9 , 1999	Forest fire	Landsat TM August 08,1999
(4)	July 13, 2000		Landsat ETM July 25, 2000

(b)

Fig. 10: (a) Spectral signature plots of burned areas and reforestation-preparation areas according to Landsat TM bands. (b) Legend for Figure 9-a.

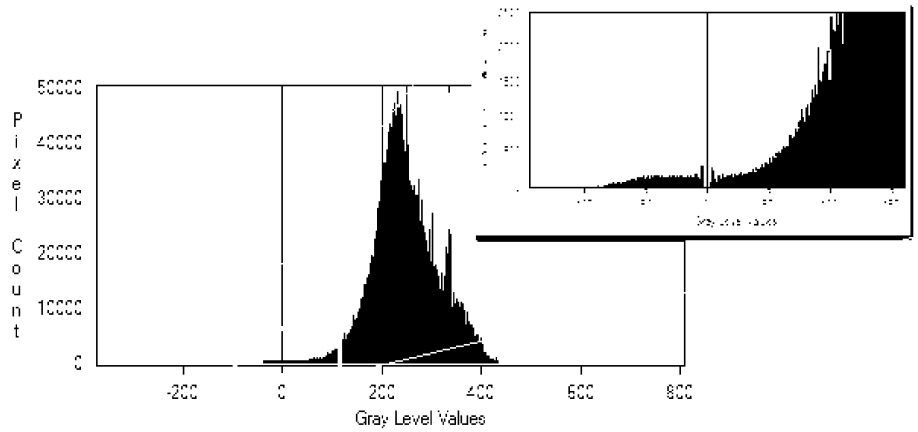

Fig. 11: The frequency histogram of pixel brightnesses for TM image dated July, 25 2000 which was used for NDTI evaluations. Fire areas correspond to the negative values of the index.

When the same calculations were repeated, in the next interval (1992 -1998), it was seen that a large portion (about 23%) of green vegetation cover was 'lost' again with a signature quite reminiscent of forest fire (Figure 6-c). There could be 2 reasons for this apparent loss: (1) another forest fire in the region, (2) clearing and preparation of the soil for a regular reforestation. We acquired the knowledge of the preparation of this soil (tillaging) for reforestation, from ÇFM.

To distinguish between (1) a forest fire area and (2) an area in preparation for reforestation, the reflectance characteristics in all bands for these two regions were re-analyzed and compared using several test areas chosen in different dates (see Figure 8). When the spectral reflections were considered (Figure 9), it was seen that the difference of TM bands 5 (NIR1) and 7 (NIR2), TM5-TM7, could help us in distinguishing these missing classes.

Actually, the "Normalize Difference Tillage Index" (NDTI) defined as in equation 2 below, makes use of this difference [1, 19]. In the next section that by use of some pre-processing with reasonable cost of time, it will be possible to find the faulty component, much faster.

$$NDTI = [(TM\ 5 - TM\ 7)/(TM\ 5 + TM\ 7)] \quad (2)$$

Here by, TM5 and TM7 are the reflectances in the Landsat TM5 (1550-1750 nm) and TM7 (2080-2350 nm) bands, respectively. Figure 10 is a representation of frequency distribution of NDTI values for the image under consideration. The analysis shows that NDTI ≤ 5 (positive values near zero or all negative values of the index) correspond to recent forest fires while NDTI > 5 (larger positive values) regions are the reforestation-preparation areas. When we apply the above results to our images, we can identify areas that look like forest fires, but actually are reforestation-preparation areas.

In the next interval from 1999 to 2001 (Figure 6-d and Table 9), it was seen that vegetation cover in 342 ha area in the 1986 forest fire area was fully grown into a forest. On the other hand, other parts of the region (about the 102 ha) have similar signatures as reforestation-preparation areas. In the last interval we have (2001 to 2007), constructive results of reforestation efforts between 1999 and 2001 were visible (Figure 6-e).

A corollary of these fires and re-forestation efforts is that a complete re-forestation interval for a tillaged area is about 6 years.

DISCUSSION AND CONCLUSIONS

It is presented specific examples of a forest fire and follow-up reforestation efforts by various image analysis methods for an interval of about 20 years between 1987-2007. Same analyses also give clues for biomass losses unrelated to forest fires, most probably, due to forest clearing for agricultural purposes.

The changes occurred in an area can usually be determined by different supervised and unsupervised classification techniques. CVA and TC methods used in this study have been significantly effective for determining the changes occurred in the amount of green vegetation. It was shown that the classification by the EM Algorithm used to distinguish the kinds of changes in the difference image is quite effective and can be used instead of other classical unsupervised classification techniques used in remote sensing change detection applications.

One type of soil/vegetation cover signature was found to be confused with forest fires when mapped in the Landsat 7, 4, 2 band combination: The reforestation-preparation in an old fire-area. Such areas are prepared for new regular forest growth. In early phases of preparations when vegetation is still small and tillage is new such areas are confused in image maps with that of (see Figure 6-a and 6-c) forest fires.

To distinguish between true forest fires and reforestation-preparation areas we can make use of so called "Normalize Difference Tillage Index" defined as in equation (2). Comparison of this image with that of regular 7, 4, 2 image allow us to distinguish the recent forest fires and reforestation-prepared areas. The index is slightly above zero or negative for forest fires while always positive for reforestation areas. NDTI can also be used to monitor land expansion efforts of by farmers. Local forest authorities can make use of this possibility through satellite images analysis techniques.

For a closer understanding of extend and the causes of forest fires, we note the following:

According to ÇFM records, the 98% of forest fires occurring in GHP has been reported to be man-made and only %2 of them were results of natural causes such as thunderstorms, lighting etc. Man-made forest fires could also classified in 2 broad cases: (a) ones due to negligence and carelessness, such as smoking cigarette, picnic fire, stubble firing, bee incense and shepherd firing; (b) fires started on purpose, such as attempting to expand the agricultural land. This latter group is probably the dominant cause. People living in these regions do attempt to expand their agricultural land and it's mist probably the cause of several small (probably also the big) forest fires. Although the GHP has been kept under close scrutiny and protection, owing to the fact that villages, agricultural fields and forests are side by side or inside each other, forest losses are not easy to prevent. The area has a very complicated structure. Furthermore the income level of the people living in this region is rather low.

There is one practice in the area which increases the risk of fire: After harvesting the crops, instead of picking up stubbles and taking away to other regions, villagers may prefer putting them into fire in their location. The stubbles that are lit easily spread over the nearby forest areas and become the cause of new fires. Windy weather prevailing in the region usually increases the burning. A closer application of Remote Sensing and GIS methods for monitoring as discussed in this communication may help to follow these incidents more closely and force the villagers to abandon such habits.

The new protection precautions as well as the education of people living in the area have vital importance to protect the forests in the GHP. New ways of getting income such as tourism should be supported as part of development planning for the region. Forest management should invest more to educate the local people about the uses of forests.

REFERENCES

1. Daughtry, C.S.T., P.C. Doraiswamy, E.R. Hunt, A.J. Stern, J.E. McMurtrey and J.H. Prueger, 2006. Remote sensing of crop residue cover and soil tillage intensity. Science Direct, Soil and Tillage Res., 91(1-2): 101-108.
2. Bruzzone, L. and D.F. Prieto, 2002. An Adaptive Semiparametric and Context-Based Approach to unsupervised Change Detection in Multitemporal Remote-Sensing Images. IEEE Transactions on Geoscience and Remote Sensing, 11(4): 452-466.
3. Kiage, L.M., K.B. Liu, N.D. Walker, N. Lam and O.K. Huh, 2007. Recent Land-Cover/Use Change Associated with Land Degradation in the Lake Baringo Catchment. Kenya, East Africa: Evidence from Landsat TM and ETM+, International J. Remote Sensing, 28(19): 4285 - 4309.
4. Olson, G.A., A. Cheriyadat, P. Mali and C.G. O'Hara, 2004. Detecting and managing change in spatial data-land use and infrastructure change analysis and detection. IEEE Xplore, 2: 729-734.
5. Huang, C., B. Wylie, L. Yang, C. Homer and G. Zylstra, 2002. Derivation of a tasselled cap transformation based on Landsat 7 at-satellite reflectance, International Journal of Remote Sensing, 23(8): 1741-1748.
6. Kauth, R.J. and G.S. Thomas, 1976. The Tasseled Cap, a Graphic Description of the Spectral-Temporal Development of Agricultural Crops as Seen by Landsat. Proc. Symp. on Machine Processing of Remotely Sensed Data. West Lafayette, Purdue University, Indiana, 41-51.
7. Flores Sánchez, E. and S.R. Yool, 2007. Sensitivity of Change Vector Analysis to Land Cover Change in an Arid Ecosystem. International J. Remote Sensing, 28(5): 1069-1088.
8. Crist, E.P. and R.C. Cicone, 1984. A Physically Based Transformation of Thematic Mapper Data: The TM Tasseled Cap. IEEE Transactions on Geoscience and Remote Sensing. 22(3): 256-263.
9. Healey, S.P., W.B. Cohen, Y. Zhiqiang and O.N. Krankina, 2005. Comparison of tasseled cap-based Landsat data structures for use in forest disturbance detection, Remote Sensing of the Environment, 97: 301-310.
10. Van Deventer, A.P., A.D. Ward, P.H. Gowda and J.G. Lyon, 1997. Using Thematic Mapper data to identify contrasting soil plains and tillage practices. Photogram. Eng. Remote Sensing, 63: 87-93.
11. Erten, E., V. Kurgun and N. Musaoğlu, 2005. Forest Fİre Risk Zone Mapping By Usİng Satellite Imagery and Gis, TMMOB Harita Ve Kadastro Mühendisleri Odasİ, 10. Türkiye Harita Bilimsel Ve Teknik Kurultayİ, 28 Mart - 1 Nisan 2005, Ankara.
12. Bovolo, F. and L. Bruzzone, 2007. A Theoretical Framework for Unsupervised Change Detection Based on Change Vector Analysis in the Polar Domain. IEEE Transactions On Geoscience and Remote Sensing, 45(1): 218-236.
13. Radke, R.J. S. andra, O. Al-Kofahi and B. Roysam, 2005. Image change detection algorithms:A Systematic Survey. IEEE Transactions on Image Processing, 14(3): 294-307.
14. Manjon-Herrera, J.V., 2006. EM Image Segmentation, Retrieved January 5,2007, From http:// www.mathworks.com/ matlabcentral/ fileexchange/ loadFile.do?objectId=10956andobjectType=file
15. Melgani, F., G. Moser and S.B. Serpico, 2002. Unsupervised change detection methods for remote sensing images. Optical Engineering, 41(12): 3288-3297.
16. D'Addabbo, A., G. Satalino, G. Pasquariello and P. Blonda, 2004. Three Different Unsupervised Methods for Change Detection: An Application, IEEE Xplore, 3: 1980 -1983.
17. Bruzzone, L. and D.F. Prieto, 2000. Automatic Analysis of the Difference Image for Unsupervised Change Detection, IEEE Transactions on Geoscience and Remote Sensing, 38(3): 1171-1182.
18. Lu, D., P. Mausel, E. Brondizio and E. Moran, 2002. Assessment of Atmospheric Correction Methods for Landsat TM Data Applicable to Amazon Basin LBA Research. International J. Remote Sensing, 23(13): 2651-2671.
19. Singh, A., 1989. Digital change detection techniques using remotely sensed data. International J. Remote Sensing, 10: 989-1003.